

# Estimation of the Inference Quality of Machine Learning Models for Cutting Tools Inspection

Kacper Marciniak<sup>1</sup><sup>a</sup>, Paweł Majewski<sup>2</sup><sup>b</sup> and Jacek Reiner<sup>1</sup><sup>c</sup>

<sup>1</sup>*Faculty of Mechanical Engineering, Wrocław University of Science and Technology, Poland*

<sup>2</sup>*Faculty of Information and Communication Technology, Wrocław University of Science and Technology, Poland*


**Keywords:** Machine Vision, Machine Learning, Tool Inspection, Tool Measurement, Inference Quality.


**Abstract:** The ongoing trend in industry to continuously improve the efficiency of production processes is driving the development of vision-based inspection and measurement systems. With recent significant advances in artificial intelligence, machine learning methods are becoming increasingly applied to these systems. Strict requirements are placed on measurement and control systems regarding accuracy, repeatability, and robustness against variation in working conditions. Machine learning solutions are often unable to meet these requirements - being highly sensitive to the input data variability. Given the depicted difficulties, an original method for estimation of inference quality is proposed. It is based on a feature space analysis and an assessment of the degree of dissimilarity between the input data and the training set described using explicit metrics proposed by the authors. The developed solution has been integrated with an existing system for measuring geometric parameters and determining cutting tool wear, allowing continuous monitoring of the quality of the obtained results and enabling the system operator to take appropriate action in case of a drop below the adopted threshold values.


## 1 INTRODUCTION

Machining is a common manufacturing method used in the industry to produce high-quality machine and equipment parts where a high degree of dimensional accuracy is crucial. Cutting tools used in mass production degrade rapidly, negatively impacting their performance in the machining process and the overall quality of the manufactured product. For this reason, tools are subjected to reconditioning, which, in the case of the hob cutters discussed in this article, involves removing a layer of material from the tooth attack face in a grinding process. Removing too little material will not fully eliminate the defect (leading to improper tool performance), while using too much allowance will significantly shorten its life (Gerth, 2012). Therefore, an accurate assessment of the degree of wear and the selection of optimal parameters for the reconditioning method becomes a critical aspect of reducing remanufacturing costs while increasing tool life significantly.

The conventional approach to solving the problem of gear hobbing tool wear estimation involves manual visual inspection of tools, which is highly inefficient and therefore, various innovative approaches have been proposed, such as analysis of CNC machine parameters using multilayer perceptron (MLP) (Wang et al., 2021) or estimation based on data from numerical simulations (Bouzakis et al., 2001), (Dong et al., 2016). Our team proposed a solution in the form of a machine vision system for inspecting the tooth rake surfaces of hobbing tools, enabling their dimensioning and unambiguous determination of the wear level of each tool after the production cycle. This system is based on machine learning image processing models, and it is therefore subject to all their limitations, such as a significant susceptibility to the variability of the input data character, which negatively impacts the model's accuracy (Szegedy et al., 2014), (Nguyen et al., 2015), (Dalva et al., 2023). This problem becomes critical when one considers how diverse the tools undergoing the scanning process are, varying in shape, dimensions, or surface quality and texture. As a solution to this problem, two fully complementary strategies can be proposed: (1) improving the robustness of the ML model to the variability of

<sup>a</sup>  <https://orcid.org/0009-0000-7098-5907>

<sup>b</sup>  <https://orcid.org/0000-0001-5076-9107>

<sup>c</sup>  <https://orcid.org/0000-0003-1662-9762>

the input data, (2) preparing a methodology to estimate the quality of the inference, which would allow the results to be evaluated and possibly rejected. This paper focuses on the second solution, based on feature space analysis methods, as this approach is highly versatile and easily applicable to other machine vision systems.

Analysing the distribution of deep data features used in machine learning is a process long familiar to researchers and data engineers. It is widely used to evaluate data distributions, determine the level of heterogeneity, and in classification tasks (Umbaugh, 2005). The method has recently begun to be utilised in the label-free evaluation of machine learning models. An example is the 'AutoEval' method (Deng and Zheng, 2020), which allows indirect determination of ML model accuracy on a given test set by analysing differences in the distribution of input and training data, calculated as Fréchet Inception Distance (FID) and referred to as distribution shift. Classification accuracy is determined using a regression model. The cited work develops a general methodology that allows application to various models or data and identifies its limitations. Analysis in feature space using the FID metric is also widely used in the Generative Adversarial Networks (GANs) evaluation process (Buzuti and Thomaz, 2023).

Considering existing research gaps in the form of a lack of practically applicable solutions for analysing and evaluating machine learning systems under industrial conditions, work was undertaken to develop a methodology for the automatic estimation of inference quality of machine learning models. The proposed solution is based on analysing the data distribution in the deep feature space and allows the level of inference quality on a given image to be determined unambiguously. It is worth noting that the proposed solution has been developed to be implemented and practically used in a simultaneously developed industrial machine vision system.

## 2 MATERIALS AND METHODS

### 2.1 Problem Definition

The problem described is the segmentation of tooth rake faces of cutting tools (hob cutters) to measure their geometric parameters, as well as the segmentation of defects such as abrasive wear (shallow damage to the surface), notching (deep tooth damage) and build-up or contamination (Figure 1). This task is non-trivial because of the significant variations of the data obtained when scanning different tools, which

Table 1: Prepared multi-domain training datasets.

Multi domain set	1	2	3	4	5	6	7	8	9
Tools	1 8 9	1 2 8	3 6 9	4 5 9	4 5 6	5 6 7	4 5 7	3 8 9	3 7 9

are due to the following: 1. variations in tool geometry between the different tool types, 2. different degrees and ways of wear depending on the working time and load of the tool, 3. the use of different protective coatings on the tools, 4. variable acquisition conditions resulting from an incorrect scanning process by the system user.

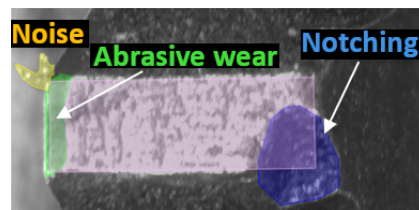


Figure 1: Examples of typical failures detected on the tooth rake face.

### 2.2 Dataset

The dataset was created using raw images of hob teeth with a dimension of 4024x3036 pixels, from which regions-of-interest (ROIs) containing tooth rake faces were cropped. The size of the cropped area was constant for a given tool type, and its values were determined by the nominal tooth length and tool pitch value.

The prepared dataset contained images of nine unique tools differing in wear, geometry and coating used (Figure 2), each containing 50 images with annotated rake faces. These sets of tooth images are referred to in the following paper as sub-domains. Each set was split in an 80/20 ratio to create independent training and test subsets. The study included nine single-domain test datasets containing approximately ten images of a single tool each and nine multi-domain training sets with three randomly selected subdomains (Table 1). This resulted in 9 unique sets of images and labels for training the test segmentation models and 9 test sets for evaluation.

### 2.3 Model Preparation

The experiment used Detectron2 implementations of the *FasterRCNN-ResNet101-FPN* (Wu et al., 2019) instance segmentation architecture with PointRend support (Kirillov et al., 2019). Each of the 19 tra-

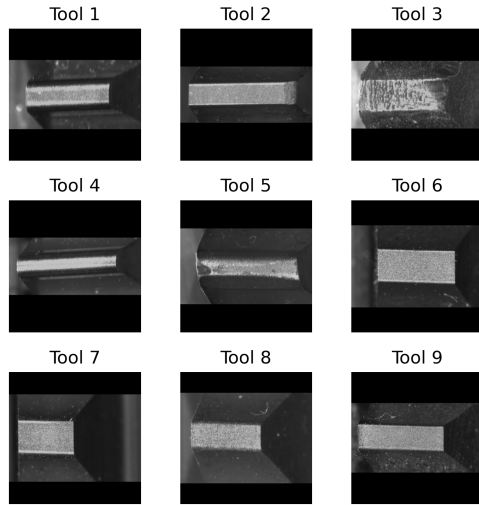


Figure 2: Example images of tools included in the dataset.

ing processes was performed with  $batch\_size = 4$  and  $epochs = 25$ , except for the final model trained on all subdomain data with a larger epoch number of 35. The number of epochs was chosen experimentally based on the analysis of data from the training process.

## 2.4 Proposed Method

The experiment proposes a comprehensive processing pipeline for both single and multi-domain sets (Figure 3), utilised in the preparation of models (instance segmentation, PCA) and data distribution metrics (mean and variance), which are subsequently used in the development of the inference quality estimator (Figure 4).

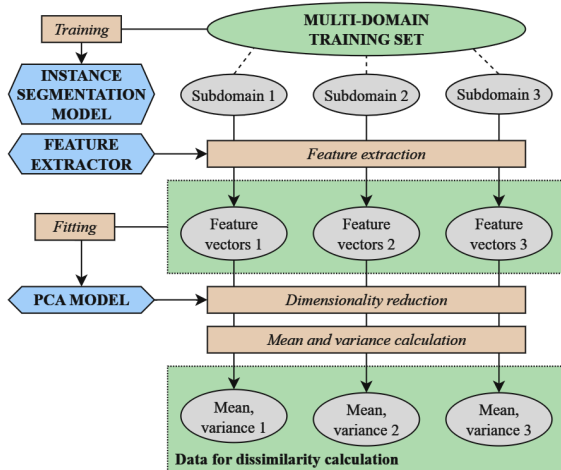


Figure 3: Proposed pipeline for model training and data analysis.

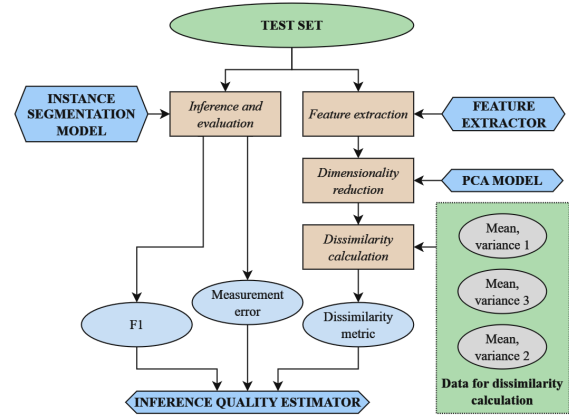


Figure 4: Model evaluation and quality estimator preparation - proposed method.

### 2.4.1 Feature Extraction

An extractor based on the pre-trained classification model with ResNet-101 architecture (He et al., 2015) and the 'IMAGENET1K\_V2' set of weights was used to extract deep features from the images. Before feature extraction, the images were transformed to a square shape by padding with black bars and rescaled to a size of 200x200 pixels. The standard normalisation procedure was applied:  $mean = [0.485, 0.456, 0.406]$ ,  $std = [0.229, 0.224, 0.225]$ . The dimensions of the resulting feature vectors were reduced using Principal Component Analysis (PCA). The PCA model was prepared based on feature vectors related to images from training sets from all sub-domains, and the output dimension was chosen to ensure that at least 99% of the training data variance was maintained.

### 2.4.2 Determination of the Level of Data Dissimilarity

The level of dissimilarity between the input image and reference set was defined as the distance in feature space between image feature vector  $F_{im}$  and data distribution defined by mean  $\mu$  and covariance  $\sigma$ . The following metrics were examined:

- Euclidean distance;
- standardised Euclidean distance (1);
- Mahalanobis distance.

$$D(F^{im}, \mu, \sigma) = \sqrt{\sum_{i=1}^k \frac{(\mu_i - F_i^{im})^2}{\sigma_i}} \quad (1)$$

Where  $k$  is the length of a feature vector.

For models trained on multi-domain sets, two ways of measuring dissimilarity have been proposed:

1. measuring the distance between the input image feature vector and the entire data distribution, 2. determining the distance as a weighted average of the distances of the image feature vector to the subdomains that form the data set (as explained on Figure 5). The weighted average is defined as follows (2):

$$D_{avg} = \frac{1}{N} \sum_{i=1}^N w_i * D(F^{im}, mean(F_i), std(F_i)) \quad (2)$$

where  $N$  is the number of subdomains and  $w_i$  is the weight determined using the average value of the F1 metric ( $F1_i$ ) obtained during the evaluation of the respective subdomain (3):

$$w_i = \frac{1.5 - F1_i^{eval}}{\sum_{i=1}^N (1.5 - F1_i^{eval})} \quad (3)$$

This approach favours subdomains with a lower F1 value, taking distances to them with more weight when calculating the dissimilarity metric.  $d_i$  is the distance between the  $i$ -th subdomain's image feature vector.

The proposed metric made it possible to assess the level of dissimilarity of the input data from the training data by determining the weighted average of the distances to each subdomain while considering the quality of the model's inference on the mentioned subdomains.

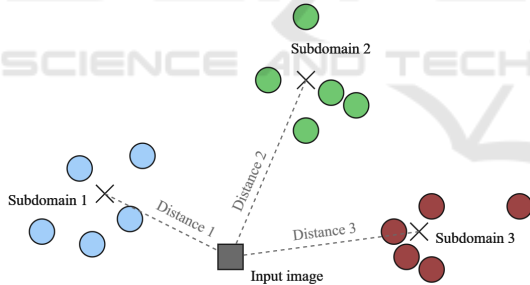


Figure 5: Proposed method of calculating distance between image and multiple subdomains in feature space.

### 2.4.3 Custom Model Evaluation

A confidence threshold of 0.75 was adopted after analysing the F1 - confidence score relationship obtained from the evaluation of the multi-domain model. The following metrics were proposed to evaluate the model for a chosen working point:

- pixel-wise F1-score (4) calculated using prediction mask ( $P$ ) and label mask ( $L$ );
- mean of absolute error of rake face width and length measurement.

$$F1 = \frac{2 * TP}{2 * TP + FP + FN}$$

$$TP = \frac{\sum(P \wedge L)}{\sum P}$$

$$FP = \frac{\sum(P \wedge \bar{L})}{\sum P}$$

$$FN = \frac{\sum(\bar{P} \wedge L)}{\sum L} \quad (4)$$

Each model was evaluated using images from the subdomain test sets - raw quality metrics (F1, measurement error) and data dissimilarity were determined. To assess the quality of the model's inference as a function of data dissimilarity, the following metrics were proposed and tested:

- cumulative average of quality metrics;
- proportion of correct predictions for a given data dissimilarity threshold;
- squared proportion of correct predictions for a given data dissimilarity threshold;

Determination of the proportion of correct predictions and measurements was carried out for 15 domain distance thresholds and boundary values of  $E_{geo}^{thresh} = 0.050$  mm and  $F1^{thresh} = 0.90$ .

## 2.5 Model Inference Quality Estimator Preparation

Based on the quality metrics from the model evaluation and the dissimilarity index of the data, the target estimator should determine the inference quality in the form of a number between 0 and 1, where 1 indicates the highest quality of the results obtained and, thus, their highest reliability. The proposed solution involves approximating the relationship of the quality metrics to the data dissimilarity index with a mathematical function and using it in the production process.

## 2.6 Effect of the Number of New Samples on the Change in the Inference Quality

In addition, work was undertaken to determine the impact of new samples in the training dataset on the quality of inference by the model. As a result, a model trained on a multi-domain data set and two single-domain test sets were selected, for which the inference quality was substantially lower. For each model-subdomain test pair, 5, 10, 20 and 40 samples were randomly selected from the training set of

the examined subdomain. These samples were used to supplement the training set and prepare a new model. The process was repeated five times, and the results were averaged. This allowed to plot the dependence of the inference quality on the subdomain on the number of corresponding samples from the subdomain in the training set.

### 3 RESULTS AND DISCUSSION

#### 3.1 Data Dissimilarity Calculation

To determine the method for calculating the data dissimilarity metric, the change in the cumulative average of  $F_1$  value as a function of domain distance was analysed (Figure 6), and the coefficients of determination for the third-degree polynomial estimation of these runs were determined. Of the analysed approaches, the Mahalanobis distance determined for both subdomains and entire data distribution proved to be the least successful, with a low coefficient of  $R^2 = 0.77$  and  $R^2 = 0.64$ . The method based on the standardised Euclidean distance with  $R^2 = 0.97$  and a shape close to the expected one was the best and was used in further work.

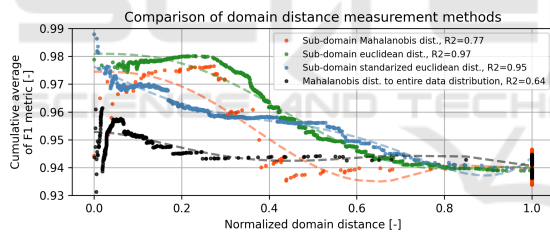


Figure 6: Comparison of different domain distance measurement methods.

#### 3.2 Inference Quality as a Function of Domain Distance

All subdomain data from the prepared dataset was put through a process of feature extraction followed by dimensionality reduction. The PCA model prepared reduced the feature vectors from 2048 to 180 dimensions, which resulted in the preservation of 99.004% of the variance. A graphical visualisation of the distribution of the deep features of the training and test sets for the first two principal components is presented below (Figure 7).

Each of the nine single-domain models, nine three-domain models and the all-domain model were evaluated on prepared test sets. The relationships presented in the graphs below were determined based on

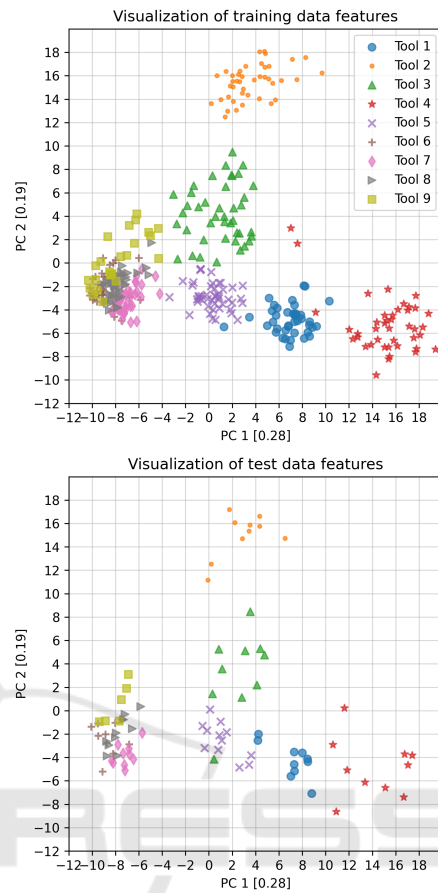


Figure 7: Visualisation of training and eval data features.

the qualitative and dissimilarity metrics obtained. Domain distance values ranging from 6.30 to 28.0 and a median of 12.5 were obtained. Values of the  $F_1$  metric ranged from 0 (no object detection) to 0.994, with a median of 0.969. For side face measurement error, values ranged from 0 to 4.97 mm, with a median of 0.047 mm. The cumulative average of the  $F_1$  metric (Figure 8) trended as expected. With an increase in the difference between the input image and the training data set (domain distance), a significant decrease in the inference quality metric was observed. It is worth noting the course of the plots, which were stair-stepping for some models - large differences in inference quality occurred when transitioning between test subdomains. The fastest decrease in inference quality as a function of domain distance was observed for models prepared using training sets consisting of images of tools 4, 5 and 6, two of which (tools 4 and 5) are significantly similar. At the same time, the lowest values were achieved for the high value of domain distance for models trained with data from tools 1, 8, 9 and 1, 2, 8.

The averaged function took a straight line shape up to a domain distance value of 20, later plateauing and holding constant at  $F_1 = 0.94$ . In this evaluation graph, the red line shows the course of the cumulative maximum value, which is one of the proposed inputs to the quality estimator being developed.

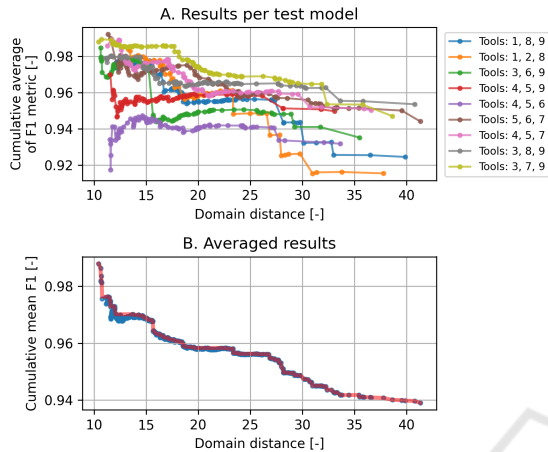


Figure 8: Cumulative average of F1 metric in the domain distance function: A. results per test model, B. averaged results.

The cumulative average of the tooth rake face dimensioning error increases with domain distance, reaching values above  $E_{geo} = 0.20$  mm for models trained on tool images 1, 8, 9 and 1, 2, 8. A significant increase in error is also observed for the set that contains similar domains 6 and 9, as well as the characteristic domain 3 (a tool with high wear and unusual surface texture). The final result was an averaged plot similar to the  $F_1$  metric, albeit with values increasing as a function of dissimilarity (Figure 9).

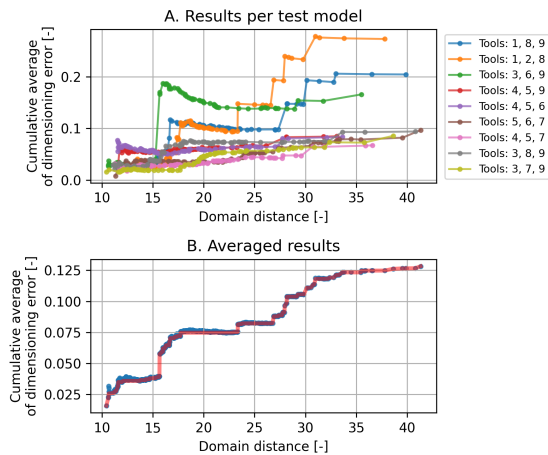


Figure 9: Cumulative average of rake face measurement error in the domain distance function: A. results per test model, B. averaged results.

When analysing the number of correct predictions and measurements, the lowest prediction performance was recorded for the model trained on sets 4, 5, 6, whilst the lowest measurement performance was observed with 4, 5, 9 (Figures 10 and 11).

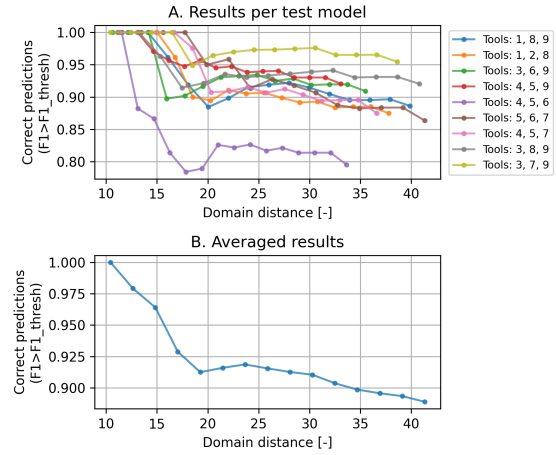


Figure 10: Proportion of correct predictions for given domain distance thresholds: A. results per test model, B. averaged results.

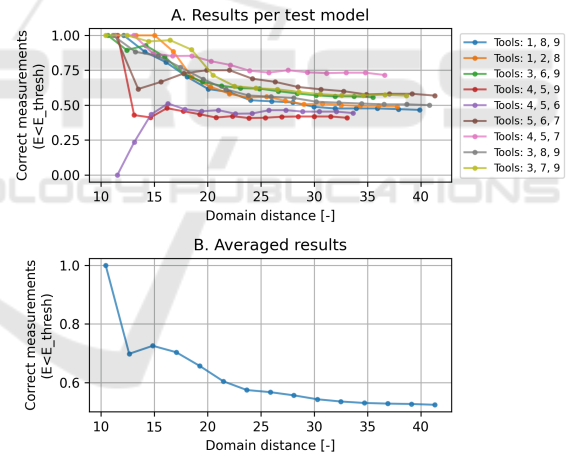


Figure 11: Proportion of correct measurements for given domain distance thresholds: A. results per test model, B. averaged results.

Any anomalies and deviations in the presented results may be due to the proposed method of determining differences between the image and input data (domain distance). Developing a metric that would unambiguously relate the differences between the distributions of deep data features and the quality of inference by the deep model is a non-trivial task. It requires further work and testing, including testing on new data sets and using other feature extractors, for example, based on our classification models.

Table 2: Effect of the number of new samples on the change in the inference quality.

New samples	AP 50:95	F1
<b>Tool 2</b>		
0	0.146	0.173
5	0.836	0.945
10	0.893	0.958
20	0.913	0.963
40	0.943	0.968
<b>Tool 4</b>		
0	0.603	0.849
5	0.696	0.917
10	0.767	0.925
20	0.786	0.933
40	0.836	0.945

### 3.3 Effect of the Number of New Samples on the Change in the Inference Quality

The model selected for the study was trained on a multidomain built from images of tools 1, 2 and 8. Images of tools 3 and 5 with inference on which the model had problems were used as test samples. In both cases, similar results were observed - the sharpest, steepest change in the quality of inference occurred when the first samples were added - for tool 2 it was a change in  $AP_{50:95}$  from 0.146 to 0.83 and  $F_1$  from 0.173 to 0.945 after adding five samples (11.9% of the available set), for tool 4: a change in  $AP_{50:95}$  from 0.603 to 0.767 and  $F_1$  from 0.849 to 0.917 for ten samples (21.3%), with subsequent changes in quality for both tools being much smaller (Table 2). The data obtained suggest that even a few samples (10) from a given domain can significantly improve the inference quality of the machine learning (ML) model. This knowledge can be used to automate the inference quality control process, where when a large difference is detected between the input data set and the training set, the system will perform a feature analysis and select a sample set for labelling, the size of which will ensure an improvement in the quality of the model's work while minimising the amount of time and effort to process and prepare the selected training data.

### 3.4 Integration with the Machine Vision Inspection System

The proposed methodology has been integrated into a developed system for cutting tool inspection. During the inference process, each input image is compared with the training set of the model used and the degree of dissimilarity is determined. This value is used to es-

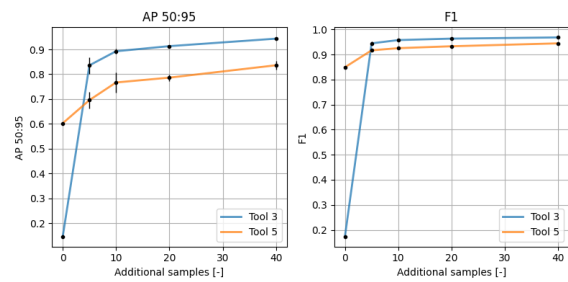


Figure 12: Experiment results for tools 2 and 4.

timate the expected level of inference quality (Figure 13). This information is communicated to the user and allows an assessment of the level of reliability of the results obtained so that appropriate action can be taken:

- accept the results obtained and use them to decide on the tool regeneration method,
- ignore or modify the results with a low level of reliability,
- stop the system and select additional training samples to prepare a new model - in the case of a critically low level of reliability.

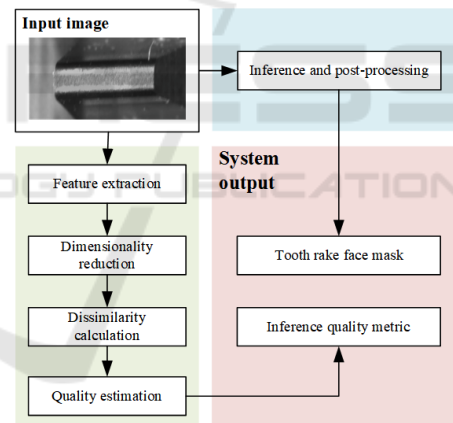


Figure 13: Conceptual scheme of the inference process.

## 4 CONCLUSIONS

The results presented in this paper showed the possibility of correlating the degree of dissimilarity of the input and training data in feature space with the inference quality metrics of the machine learning model. This demonstrates the potential of using this approach to estimate the performance quality of ML-based machine vision systems in production environments. Such a solution is very much needed for systems with high input data variability. An example would be cutting tool wear assessment equipment, where the results' quality can be significantly and negatively af-

ected every time the tool parameters change. A system based on the proposed methodology would allow not only the assessment of the reliability of inference results but also the automation of the process of training data selection by indicating the optimal number of samples needed.

The machine learning models deployed as part of this experiment respond differently to the variability of the deep features extracted from input images, showing high robustness even to significant changes in some of them while simultaneously being highly sensitive to others. For this reason, further work would be required to improve the proposed methodology for determining the degree of dissimilarity of the data by developing methods that are less general and closely related to the character of the processed data. The considered approaches are the use of feature extractors based on image classifiers trained on images of cutting tools acquired with the developed vision system or direct determination of inference quality with the use of a regression model.

## ACKNOWLEDGEMENTS

We want to thank Wojciech Szelaĝ and Mariusz Mrzyĝłod from the *Wrocław University of Technology*, who took an active part in the development and construction of the machine vision system used, as well as the staff at *TCM Poland* for providing the materials necessary to carry out the work described in this paper.

## REFERENCES

- Bouzakis, K.-D., Kombogiannis, S., Antoniadis, A., and Vidakis, N. (2001). Gear Hobbing Cutting Process Simulation and Tool Wear Prediction Models. *Journal of Manufacturing Science and Engineering*, 124(1):42–51.
- Buzuti, L. F. and Thomaz, C. E. (2023). Fréchet autoencoder distance: A new approach for evaluation of generative adversarial networks. *Computer Vision and Image Understanding*, 235:103768.
- Dalva, Y., Pehlivan, H., Altundiş, S. F., and Dundar, A. (2023). Benchmarking the robustness of instance segmentation models. *IEEE Transactions on Neural Networks and Learning Systems*, pages 1–15.
- Deng, W. and Zheng, L. (2020). Are labels necessary for classifier accuracy evaluation? *CoRR*, abs/2007.02915.
- Dong, X., Liao, C., Shin, Y., and Zhang, H. (2016). Machinability improvement of gear hobbing via process simulation and tool wear predictions - the international journal of advanced manufacturing technology.
- Gerth, J. L. (2012). *Tribology at the cutting edge: a study of material transfer and damage mechanisms in metal cutting*. PhD thesis, Acta Universitatis Upsaliensis.
- He, K., Zhang, X., Ren, S., and Sun, J. (2015). Deep residual learning for image recognition.
- Kirillov, A., Wu, Y., He, K., and Girshick, R. (2019). PointRend: Image segmentation as rendering.
- Nguyen, A., Yosinski, J., and Clune, J. (2015). Deep neural networks are easily fooled: High confidence predictions for unrecognizable images. In *Proceedings of the IEEE Conference on Computer Vision and Pattern Recognition (CVPR)*.
- Szegedy, C., Zaremba, W., Sutskever, I., Bruna, J., Erhan, D., Goodfellow, I., and Fergus, R. (2014). Intriguing properties of neural networks.
- Umbaugh, S. (2005). *Computer Imaging: Digital Image Analysis and Processing*. A CRC Press book. Taylor & Francis.
- Wang, D., Hong, R., and Lin, X. (2021). A method for predicting hobbing tool wear based on cnc real-time monitoring data and deep learning. *Precision Engineering*, 72:847–857.
- Wu, Y., Kirillov, A., Massa, F., Lo, W.-Y., and Girshick, R. (2019). Detectron2. <https://github.com/facebookresearch/detectron2>.